SENSORY-MEDIATED TRACKING BEHAVIOUR IN TURBULENT CHEMICAL PLUMES

Donald R. Webster
School of Civil & Environmental Engineering
Georgia Institute of Technology
790 Atlantic Drive, Atlanta, GA 30332-0355 USA
dwebster@ce.gatech.edu

Konstantin Y. Volyanskyy
School of Civil & Environmental Engineering
Georgia Institute of Technology
790 Atlantic Drive, Atlanta, GA 30332-0355 USA
kv32@mail.gatech.edu

Marc J. Weissburg
School of Biology
Georgia Institute of Technology
310 Ferst Drive, Atlanta, GA 30332-0230 USA
marc.weissburg@biology.gatech.edu

ABSTRACT

We designed and implemented a series of signal processing routines and feedback control algorithms for sensor-mediated chemical plume tracking in a turbulent flow environment. In our design, we focused on development of a signal processing strategy capable of replicating behavioural responses of actively tracking blue crabs (*Callinectes sapidus*) to chemical stimuli. We have developed a command generation unit for sensor-mediated tracking the source of a turbulent chemical plume via motion in two directions (i.e., forward-back and left-right). Upstream motion is induced by a binary response to supra-threshold spikes of concentration and cross-stream steering is controlled by contrast between bilaterally-separated sensors. Like animal strategies, the developed control algorithm is dynamic in nature. This property allows the algorithm to function effectively in the highly irregular turbulent environment and produces adaptive adjustments of motion to minimize the distance to the source of a plume. Preliminary trials indicate that roughly 80% of the tracks successfully end near the plume source location.

INTRODUCTION

Chemosensation is an important sensory mode for animals, allowing them to locate food, mates, or predators. A major hindrance to understanding chemically-mediated guidance is the difficulty of quantifying the relevant signal properties of chemical stimulus plumes. The presence of turbulent flow fluctuations at large Reynolds number creates a spatially and temporally complex chemical environment. The characteristics of odorant plumes in such environments cannot be predicted via analytical methods (e.g., turbulent diffusivity models) or simple numerical simulations. Hence, a major challenge in understanding chemosensory-mediated guidance is to quantify the characteristics of the chemical signal structure and the signal transport in turbulent environments.

Plumes develop when flow transports chemical compounds downstream while turbulence stirs and mixes concentration filaments to expand the plume and dilute the concentration (Webster 2007). The result is a complex spatial and temporal concentration pattern (Figure 1). Fine filaments of odorant concentration within the plume are separated by unscented fluid. Animals must use these complicated patterns to navigate to a chemical source. This requires three sequential processes — making contact with the plume, using information in the chemical plume structure to move toward the source, and determining when the source has been reached. This sequence is used by many organisms, including moths, lobsters, crayfish, and blue crabs, to locate food, mates, and other items over distances of 10's to 100's of body lengths.

In contrast to the high performance displayed by animals, we have yet to develop good tracking strategies for use in autonomous unmanned vehicles (AUVs) that track turbulent chemical plumes. Traditional sensing approaches, such as time-integration to compute average properties, fail in turbulent plumes due to the high spatial and temporal variability of the chemical signal. Nevertheless, there have

been several attempts at chemically-mediate tracking strategies (e.g., Ishida et al. 1999, Grasso et al. 2000, Farrell et al. 2005), mostly inspired by analysis or observation of animals. The best strategies use some of the principles employed by animals, especially terrestrial and aquatic arthropods (i.e., moths and crabs or lobsters), which have developed sensing mechanisms that are well-matched to the properties of turbulent chemical plumes.

Figure 1. Flow visualization of the chemical plume, which is created via a continuous iso-kinetic release of a dye solution into a fully developed turbulent boundary layer. The view is from above, with the flow moving from left to right (Page et al. 2011a).

Our goal is to develop a feedback control algorithm to autonomously track turbulent chemical plumes and identify the plume source with a high degree of success and low rate of false detection. With a solid understanding of the turbulent scalar field characteristics and information content in chemical plumes, we can develop and test sensor-mediated algorithms for tracking chemical plumes based on our analysis of how animals extract information from such signal environments. To this goal, we developed a test bed that can evaluate the general feedback control mechanisms that enable effective tracking using information from turbulent chemical plumes.

BACKGROUND

This section focuses on the second phase of the tracking problem: extracting information from the plume structure in order to move successfully toward the source. Animal performance indicates that they are effectively extracting useful information from the structure of chemical plumes. The basic question is: what information in the intermittent and chaotic plume structure is providing cues to guide tracking?

Information in Turbulent Chemical Plumes

Figure 1 shows a photograph of a chemical plume in a turbulent water flow. The effluent has been released from a small orifice at the left (upstream) edge of the photograph. The filament forms an irregular pattern that wanders randomly across the image, which is evidence of the turbulent stirring process. The concentration within the filament is clearly more dilute in some regions compared to others. The concentration distribution shows a complex pattern in space, which is continually evolving. Advances in experimental technology in the past decade have provided valuable quantitative insight to the spatial and temporal variation of chemical plumes in the aquatic turbulent environment (e.g., Webster & Weissburg 2001, Crimaldi et al. 2002). For instance, laser-induced fluorescence (LIF) is an optical measurement technique that yields sequences of the instantaneous concentration spatial distribution (Webster et al. 2003). Figure 2 shows a quantitative example of the three-dimensional plume structure. This figure demonstrates the significant spatial variation in the chemical plume structure. The instantaneous structure of the concentration field is continuously evolving in time as well, although this fact is not apparent in Figure 2.

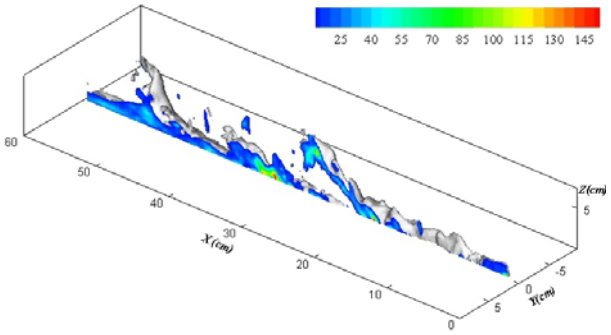

Figure 2: Sample instantaneous concentration field measured via three-dimensional laser-induced fluorescence (3DLIF). The colour contours indicate the local concentration in a vertical plane at the plume centreline. The grey contour corresponds to a small concentration level and effectively denotes a three-dimensional outer boundary of the plume structure. The chemical source is located at $x = 0$ and $y = 0$ and the release is iso-kinetic into a full developed turbulent boundary layer. The flow direction is in the positive x-direction.

The smooth and predictable gradient in the time-averaged concentration field seems useful for tracking at first glance (Figure 3). A tracker would simply move up the concentration gradient by comparing sequentially the response of a single sensor to eventually locate the position of the highest concentration, which is coincident with the source. This strategy is called chemical klinotaxis, and small organisms, such as bacteria and nematodes, are believed to employ this strategy in laminar flow environments (reviewed in Webster and Weissburg 2009). Unfortunately, this strategy is ineffective for rapid tracking of turbulent chemical plumes for the simple reason that the information shown in Figure 3 is unavailable. The time period necessary to determine the time-averaged concentration with sufficient accuracy to perceive the gradient direction is many minutes (Webster and Weissburg 2001). To follow the gradient in Figure 3, a tracker would have to collect chemosensory information for several minutes at a specific location, compare the estimated concentration to the time-averaged concentration previously collected to assess the gradient direction, and then move and start the process again. Blue crabs are observed to track

distances of roughly 2 m in 30 seconds or less, which is inconsistent with a slow sampling strategy that compares time-averaged concentration values.

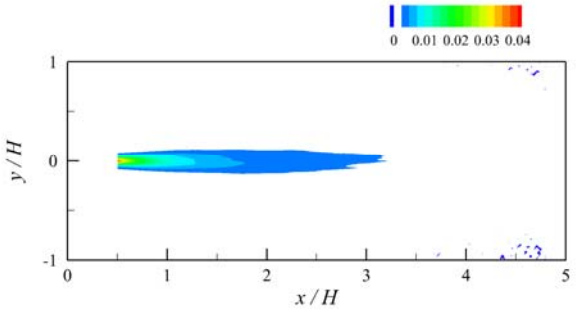

(a)

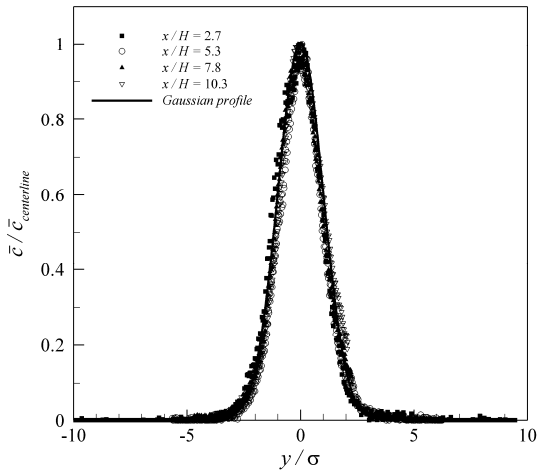

(b)

Figure 3: (a) Time-averaged concentration field in a horizontal plane at the same height as the source nozzle. The contour values are normalized by the source concentration. (b) Cross-stream profiles of the time-averaged concentration at four downstream locations. The profiles are self-similar and the solid line corresponds to a Gaussian profile shape (Webster 2007).

Figure 4 demonstrates that the convergence of the time-averaged concentration calculation takes roughly 10 minutes for the example plume. To generate this figure, the total time record (example segment shown in Figure 5) was divided into numerous shorter periods, and the time-averaged value was calculated for each of the sub-periods. For sample periods of 4.7 seconds, for instance, the time-averaged values vary by a huge range, roughly 200% larger to 100% smaller than the converged value. Thus, to accurately assess the concentration value compared to the concentration at the previous location, a much longer sampling period is needed. The data scatter is not solely a result of the number of samples that are collected, as one might expect from statistical considerations. Rather, it results directly from the intermittent nature of the concentration field. In other words, a sensor must sample over a time period sufficient for numerous filaments to pass by in order to determine a converged time-averaged value. Thus, the intermittent nature of the concentration field necessitates very long sampling periods in order to evaluate any time-averaged quantity, including the time-averaged concentration shown here. Obviously, a strategy that employs the gradient in a time-averaged quantity is extremely tedious. It is clear that blue crabs and other organisms are employing strategies that are much more efficient than waiting for time-averaged quantities to statistically converge. Thus, they appear to be acquiring information from the fluctuating plume structure.

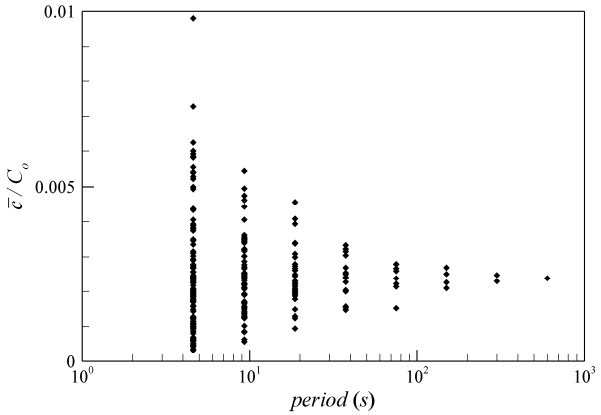

Figure 4: Time-averaged concentration as a function of sampling period at an arbitrary location in the flow. The total time record of 600 seconds was divided into numerous shorter periods to demonstrate the slow convergence of the time-averaged concentration calculation (Webster and Weissburg 2001).

Several hypotheses have been suggested about the nature of the sensory information available in turbulent chemical plumes. For instance, Moore and Atema (1991) reported that the rise slope of a concentration burst (see time record in Figure 5) varies with distance from the source, and hence provides ranging information during tracking. Webster and Weissburg (2001) confirmed that the time-averaged value of the rise slope changes systematically as a function of distance from the source. However, like the concentration value, the rise slope at any location varies unpredictably and a long sampling period is required to achieve a converged time-averaged value. This is, in fact, the underlying problem with any cue that requires time-averaging: the convergence time in an intermittent plume is very long and the required monitoring prevents rapid tracking progress. The instantaneous concentration or rise slope at a particular location in the plume is any value within a broad range, and hence does not provide predictable information.

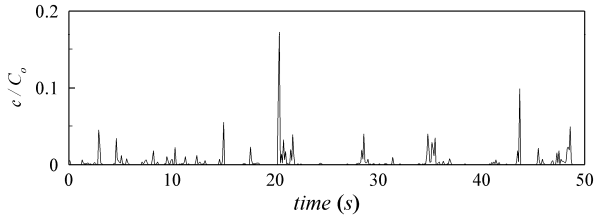

Figure 5: Sample time record of concentration at a point along the plume centreline. The instantaneous concentration is normalized by the source concentration (Webster 2007).

Tracking Strategies

Current approaches to autonomous chemically-mediated guidance in turbulent plumes fail to capitalize on new knowledge regarding animal sensing and have only incorporated the most basic elements seen in animal strategies. Improvements in several areas are necessary, and possible, given existing information. For instance, there has been little attention paid to the spatial arrangement of sensors in relation to the navigational tasks they perform and to differences in the type of information that can be extracted from sensors in different locations. Our analysis indicates that blue crabs use two sets of chemosensors that are responsible for regulating different aspects of the organism's tracking behaviour (Keller et al. 2003), and blue crabs do so by taking advantage of chemical plume structure at different elevations in the water column (Jackson et al. 2007). Chemosensors on the antennules, which are elevated on the crab's body, control the forward movement of the crab via odor-gated-rheotaxis (a strategy whereby odorant arriving at these sensors is coupled with mechanosensory information to induce upstream motion towards the odorant source). Chemosensors on the crab's legs, which are spatially separated and near the substrate, are believed to mediate turning relative to the plume structure. The combination of sensors at different heights in the water column means that blue crabs are acquiring time-varying, three-dimensional (3D) information about their environment.

We used a three-dimensional laser-induced fluorescence (3DLIF) system to collect chemical concentration data simultaneously with behaviour observations of actively tracking blue crabs in a variety of plume types, and sampled near both sensor populations. (Dickman et al. 2009). An example of the concentration field data surrounding an actively tracking blue crab is shown in Figure 6. The simultaneous data allow us to directly link chemical signal properties at the antennules and legs to subsequent upstream and cross-stream motions while altering the spatial and temporal intermittency characteristics of the sensory field. Figure 7 shows an example of simultaneous time records of the extracted maximum concentration near the antennules and crab kinematic parameters.

Our results suggest that chemical stimuli elicit responses in a binary fashion by causing upstream motion provided the concentration at the antennules exceeds a specific threshold (Page et al. 2011a). In particular, we observe a significant association between animal velocity changes and odorant spike encounters defined using a threshold that is scaled to the average of the instantaneous maximum concentration in the vicinity of the antennules. Thresholds are different for each crab, indicating a context-sensitive response to signal dynamics. Our data also indicate that high frequency of chemical spike encounters terminates upstream movement. Further, the data provide evidence that the previous state of the animal and prior stimulus history influence the behavioural response (i.e., the response is context dependent). Two examples are: (1) crabs receiving prior chemical spikes attain elevated velocity more quickly in response to subsequent spikes; and (2) prior acceleration or deceleration of the animal influences the response time period to a particular chemical spike. Finally, sensory information from the leg and antennule chemosensors interact, suggesting parallel processing of chemical spike properties during navigation (Page et al. 2011a).

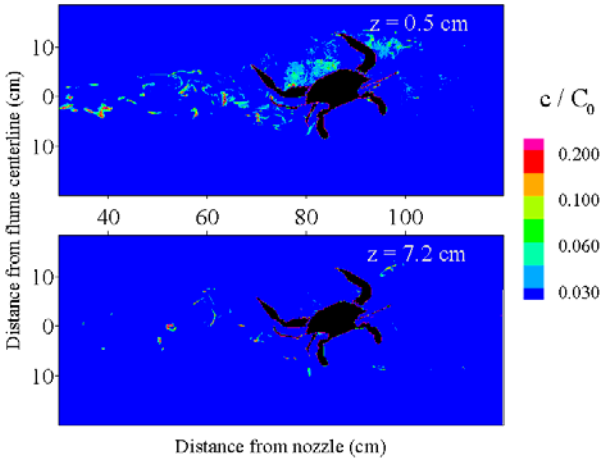

Figure 6. Concentration fields around an actively tracking blue crab shown at two elevations corresponding to approximately the height of the leg chemosensors (z = 0.5 cm) and antennule chemosensors (z = 7.2 cm) (Dickman et al. 2009).

The 3D concentration fields also facilitate a consideration of the role of broadly-distributed sensor populations in chemosensory searching, especially cross-stream heading adjustment. Our analysis indicates that the spatial distribution of the chemical concentration field is necessary and sufficient to mediate correct cross-stream motion, although concentration magnitude provides information that supplements that obtained from the spatial distribution (Page et al. 2011b). Crabs detect and respond to shifts in the cross-stream position of the centre-of-mass of the chemical concentration distribution as small as 5% of the leg span, which corresponds to roughly 0.8 – 0.9 cm. The reaction time after an above threshold shift in the position of the centre-of-

mass is in the range of 2 – 4 s. The data also indicate that these steering responses are dependent on stimulus history or other characteristics of the plume, with animals taking longer to respond in conditions with large-scale spatial meanders (Page et al. 2011b).

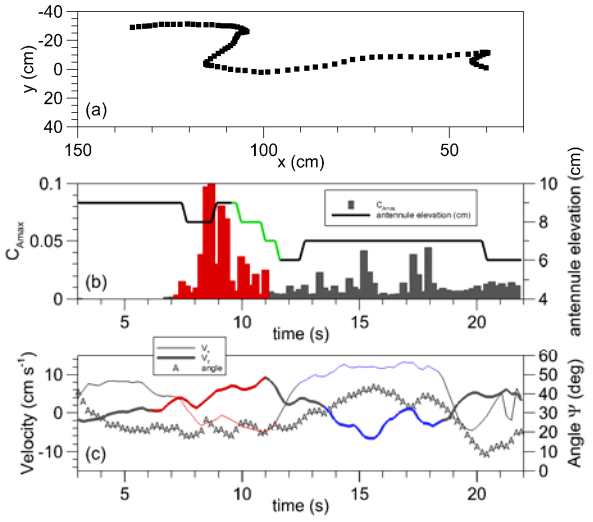

Figure 7: Example of extracted time records for a blue crab in a meandering plume. (a) Crab trajectory with data points separated by 0.21 s, (b) concentration and antennule elevation data and (c) along-stream and cross-stream walking velocities and crab orientation angle data. High concentration bursts, shown in red, occurred after the crab moved in the cross-stream direction (also shown in red in c). The interception of the high concentration bursts resulted in a lowering of the crab antennules by ~2.5 cm (shown in green). The crab moved rapidly upstream (shown in blue) after the cross-stream and vertical adjustments while making cross-stream adjustments in the opposite direction of those shown in red (Page et al. 2011a).

These detailed biological and physical observations are supported by computer simulations of search behaviour operating in a digital environment consisting of concentration fields recorded via laser-induced fluorescence (Weissburg and Dusenbery 2002). The simulations demonstrate that a simple rule-based algorithm combining odor-gated-rheotaxis and chemo-tropotaxis (i.e., cross-stream position adjustment based on spatial comparison of chemical signals) is sufficient to explain blue crab movements toward the source. The relative weighting of odor-gated-rheotaxis and cross-stream steering substantially changes tracking performance, which indicates the importance of both sources of information for successful tracking behaviour. This can be explained with the following examples. By underweighting of the cross-stream steering component, the tracker lacks sufficient ability to move toward the plume centreline and consequently loses contact with the plume and potentially moves past the source location. Conversely, underweighting the odor-gated-rheotaxis component leads to confusion about the upstream (i.e. source) direction and consequently trackers fail to make consistent progress in the source direction.

METHODS & MATERIALS

Experimental trials were conducted in a 1.07 m wide, 24 m long tilting flume. A submerged pump delivered water to the head box of the tilting flume from an underground sump. Stilling devices in the head box conditioned the flow entering the flume to be spatially uniform with low turbulence intensity. The tailgate position and bed slope were adjusted to create uniform depth flow conditions (to within 0.3 mm). For the measurements reported here, the average channel velocity, *U*, was 50 mm/s and the flow depth, *H*, was 200 mm. The boundary layer characteristics for these flow conditions were previously reported in Rahman and Webster (2005).

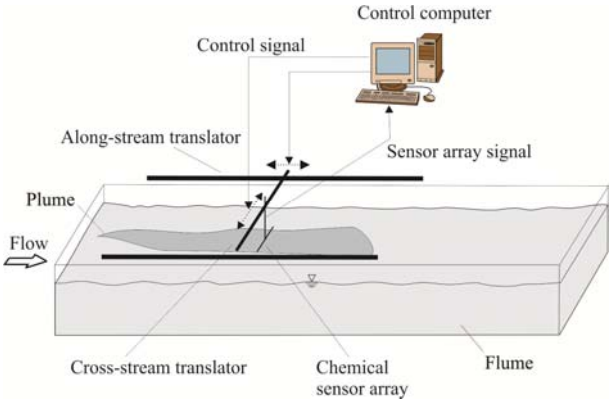

Figure 8. Schematic of the algorithm testing apparatus. The two-axis linear translator system is interfaced to the control computer, which acquires sensor input from up to 5 sensors on the sensor array.

The tracking system processes chemical sensor signals and autonomously moves the sensor array (Figure 8). The system allows us to focus on developing sensing strategies (as opposed to motion control) by avoiding implementation on a robotic platform. The motor actuators, which consist of linear translators, are easy to control and allow independent motion in two directions. The linear translator system was constructed by Parker Automation and consists of motor-driven rodless actuators aligned with the along-stream and cross-stream directions (photograph shown in Figure 9). The motor controllers accept command strings to guide their motion. The cross-stream span of the system is 1 m, and the along-stream length is 2 m, with actuator speeds that allow the device to move at rates of up to 15 cm/s (equivalent to blue crabs). In the current configuration, the step size is a coarse 10 cm.

We employ fast conductivity sensors (Precision Measurement Engineering, Inc.) to develop tracking

algorithms because they provide spatial (0.5 mm) and temporal (up to 800 Hz) resolution that allows us to replicate animal capabilities. The plume source consists of a neutrally-buoyant salt (NaCl) water solution released into the fully developed turbulent boundary layer via a small (4.2 mm diameter) nozzle (isopropyl alcohol is added to the salt solution to create neutral buoyancy). The release nozzle is located 3.8 cm above the flume bed with the iso-kinetic release pointed downstream. This duplicates previous methods, hence provides a well understood chemical stimulus environment (e.g., Webster and Weissburg 2001, Webster et al. 2003, Rahman and Webster 2005) in which to test our sensor-mediated strategies and facilitates comparisons with blue crabs tested in the same conditions (e.g., Keller et al. 2003, Jackson et al. 2007, Page et al. 2011a,b). The arrangement of the three conductivity sensors is inspired by the geometric arrangement of the antennule and leg chemosensors on blue crabs. Two sensors are broadly separated in the cross-stream direction (12.5 cm separation) and positioned 7.5 cm above the flume bed. The third sensor is located higher (12.5 cm) above the flume bed and is centred in the cross-stream direction.

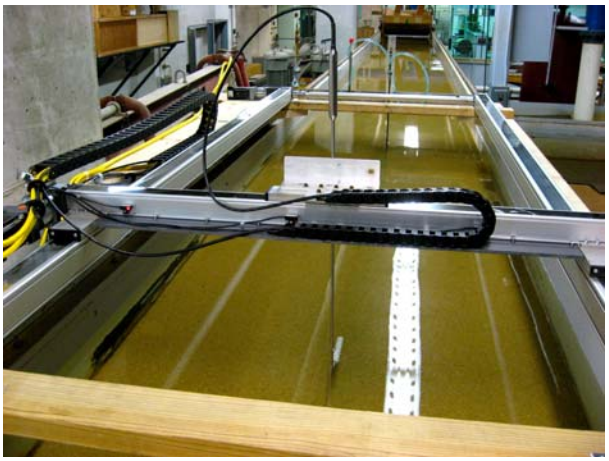

Figure 9. Photograph of the apparatus installed on the 24 m long tilting flume. The perspective is looking in the upstream direction. One conductivity sensor is installed for this example.

The sensor signal (output as voltage) is collected by the control computer and applied to the rule-based tracking algorithm (described below) that commands the linear translators to move the sensor array. The analog-to-digital signal collection is performed with a multi-purpose DAQ module with 8 A/D (range -5 to 5 V) channels available (National Instruments). Sensor data was collected at 20 Hz, which provided a good balance between rapid sample update rate and minimizing signal noise. The data acquisition and tracking algorithm is programmed in MATLAB™. Commands are sent to the linear translator controllers via Ethernet Communication Interface and are initiated by C++ code (which interfaces with the primary MATLAB™ code).

DESCRIPTION OF TRACKING ALGORITHM

The sensor-mediated tracking algorithm consists of the following elements:

- *Data Acquisition Unit*
- *Relative Position/Data Builder*
- *Spike Record Analyzer*
- *Threshold Analyzer*
- *Spike Characteristics Predictor*
- *Short-Term Input-Output History Analyzer*
- *Neuroadaptive Learning-Based Command Generator*
- *Decision Unit*
- *Motion Command Generator*

During operation, the tracker is performing forward and cross-stream motions in search of the direction of the spike magnitude increase. Cross-stream motion may be performed to gather concentration statistics and estimate the location of the plume centreline location. Motion commands are generated by the *Neuroadaptive Learning-Based Command Generator* and sent to the motion control system through the *Decision Unit*. The search algorithm is based on a binary threshold paradigm, where the threshold is estimated adaptively during the search process by the *Threshold Analyzer*. Motion commands depend on the estimation of spike sequence characteristics (spike magnitude, spike standard deviation, spike frequency, mean inter-spike interval, and current stage of motion). The *Decision Unit* maps the input signal pattern to the appropriate class of response replicating the likely response of a blue crab. The purpose of the *Relative Position/Data Builder* is to construct a data map of the performed motions and corresponding measurements and store these data in the long-term memory. This is required since we use variable threshold rules, hence information on movement history and current position enables us to employ these rules based on the current position of the sensor platform. The *Spike Characteristics Predictor* uses short-term memory data to predict the characteristics of a one-step-ahead measurement. The *Spike Characteristics Predictor* output is used to compute a prediction error which is sent to the *Short-Term Input-Output History Analyzer* and subsequently used in the *Neuroadaptive Learning-Based Command Generator*.

The algorithm is given below:

Step 0:

- Initialize relative position (*Relative Position/Data Builder*) and prediction error (*Spike Characteristics Predictor*)
- Perform an initial cross-stream sweep

Step 1:

- Measure concentration at each sensor (*Data Acquisition Unit*)

Step 2:

- Update measurement history (*Relative Position/Data Builder*)

Step 3:

- Compute short-term signal characteristics: average spike magnitude, average spike standard deviation, average spike rate, mean spike interval, and threshold estimate (*Spike Record Analyzer, Threshold Analyzer*)
- Compute Prediction Error (*Spike Characteristics Predictor*)
- Identify if below or above threshold (*Short-Term Input-Output History Analyzer*)
- Generate threshold analysis report (*Short-Term Input-Output History Analyzer*)
- Generate input-output analysis report (*Short-Term Input-Output History Analyzer*)
- Estimate position relative to the source (*Short-Term Input-Output History Analyzer*)
- Check if Stopping Condition is satisfied (*Decision Unit*). If yes, stop. If no, go to Step 4

Step 4:

- Compute direction, speed, and acceleration of the next motion (*Neuroadaptive Learning-Based Command Generator, Decision Unit*)

Step 5:

- Generate the motion command (*Decision Unit*)

Step 6:

- Update command history (*Relative Position/Data Builder*)
- Update relative position (*Relative Position/Data Builder*)
- Send the motion command to the motion controller (*Motion Command Generator*) and go to Step 1

In the *Spike Record Analyzer*, a spike is defined as a sample in the record for which the two neighbouring samples (i.e., previous and next) have smaller magnitude (Figure 10). During data processing and spike identification a minimum threshold value of -4.98 V is applied to exclude noise from subsequent analysis. Furthermore, a dynamic threshold value is computed based on $C_{avg}/2$ rule (see Page et al. 2011a), which consists of defining the threshold based on half of a running average of the spike concentration values. Only spikes that exceed this threshold value are considered in further analysis (Figure 10).

Upstream motion is governed by the analysis of the short-term history of the concentration measurements (*Short-Term Input-Output History Analyzer* and *Decision Unit*). Upstream motion is activated if the average spike magnitude has increased since the last upstream motion step. "Average" means time average over the period since the previous step, and the centre probe has greater weighting for this function compared to the other probes. Each value of the average spike magnitude is compared with the predicted value (discussed further in the Results section). The prediction error is used to adaptively adjust direction, speed, and acceleration of the next move. In addition, after each full cross-stream sweep (initial or when plume signal is lost) and corresponding identification of the cross-stream position with the greatest concentration, the tracker moves one step upstream relative to the location of that position.

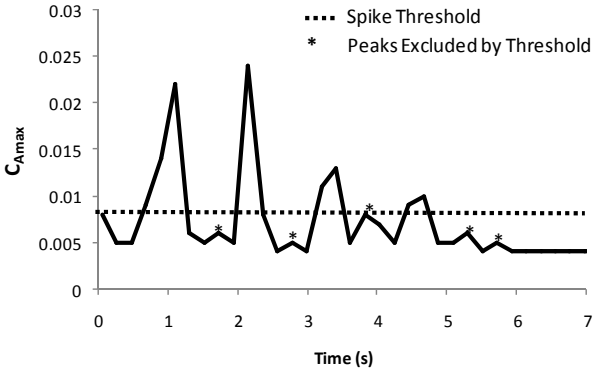

Figure 10: Example time record of concentration signal for a crab tracking in a turbulent chemical plume. C_{Amax} represents the instantaneous concentration in the region near the antennule chemosensors. Spikes are indentified as samples with greater magnitude than the previous and next samples. Spikes that exceed the illustrated threshold are included in further analysis (Page et al. 2011a).

Control of cross-stream motion is essential for plume tracking since correct identification of the cross-stream location of maximum concentration has immediate impact on the "correctness" of upstream motions and eventually on the success of the tracking as well as tracking performance measures (final distance to the source, search time etc.). This type of motion is performed in the initial step (first tracker motion), and later adjustments of the cross-stream tracker position with respect to the plume (*Short-Term Input-Output History Analyzer* and *Decision Unit*). The cross-stream motion is directed by the steering algorithm based on contrast analysis of the measurements detected on the two steering probes (i.e. leftmost and rightmost probes). Cross-stream motion is actuated if the contrast between the measurements on the two steering probes exceeds a specified threshold value. The non-steering probes can suppress cross-stream motion; if an upstream motion was performed on a previous step and the time-averaged concentration detected on a non-steering probe is sufficiently greater than the similar measurement on the previous step, then the next step involves upstream motion without any cross-stream motion regardless of the possible contrast in the measurements of the steering probes.

RESULTS

Threshold Identification

We ask whether the rules we have identified from observing blue crabs will work to extract distance and direction information as the sensor platform moves. Specifically, we seek to confirm that the proposed adaptive-threshold rule will work. Toward this goal, we performed a number of experiments in which we measured the fluctuating chemical concentration with the conductivity probes at

different locations from the source. We identified several findings that are important for further algorithm development.

First, the most descriptive statistics of the signal are: spike average magnitude (Figure 11), spike standard deviation (Figure 12), and spike frequency (Figure 13). In particular, we observed that the spike average magnitude shows an exponential-like decrease with distance from the source (Figure 11). Spike standard deviation has a similar trend of exponential-like decrease with the distance from the source (Figure 12). Spike frequency has a tendency to increase with the distance from the source without any particular identifiable functional dependence (Figure 13).

Second, we are able to predict a threshold value for every distance from the source in the range of 0 to 200 cm downstream. Via interpolation of data at distances of 10 cm, 50 cm, 100 cm, 150 cm, and 200 cm we are able to estimate the characteristic exponential dependence of the threshold versus distance using the $C_{avg}/2$ rule.

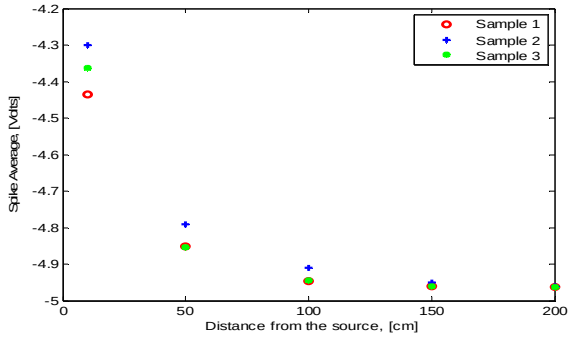

Figure 11: Three replicates of the spike average magnitude [Volts] as a function of distance from the source.

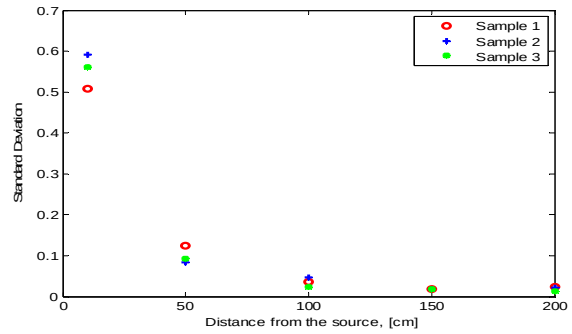

Figure 12: Three replicates of the standard deviation of fluctuations of the spike concentration [Volts] as a function of distance from the source.

These results indicate that a binary rule based on movement in response to above threshold spikes will allow efficient progress to the source. The initial threshold is based on the plume-specific parameters far from the source and is updated as the tracker moves forward in order to account for the tendency of the concentration spikes to increase. This results in a strategy that is robust to changing conditions since the determination of what represents a salient stimulus (e.g., chemical spike) is contingent on local information. Other parameters such as standard deviation can augment the binary threshold rule and directly encode information about distance to the source.

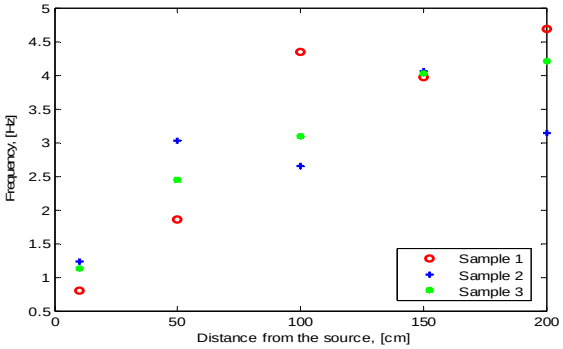

Figure 13: Three replicates of the frequency of concentration spike arrival [Hz] as a function of distance from the source.

Preliminary Tracking Trials

Figure 14 shows an example of a successful track performed by the sensor-equipped tracker. The tracker initially performs a complete cross-stream sweep. It then returns to the identified location of the greatest concentration and makes one step forward. At the new location, the recorded average spike magnitude value is less than at the previous step, and hence, the tracker performs one cross-stream step to the right and then a two-step move to the left. During this period, the recorded average spike magnitude is still less than the average spike magnitude one step downstream. The tracker concludes that it has lost the plume, and again performs a full cross-stream sweep. Having identified the location of greatest average spike magnitude, it then makes one step forward. In this step, it observes greater average spike magnitude and makes one upstream step again. It then continues to make upstream steps, as long as the average spike magnitude values increase with each step. At some point the tracker performs another left-and-right cross-stream motion sequence, and subsequently one right cross-stream step. After these two steps it continues to move upstream near the plume centreline. With the spike frequency reaching a threshold, the tracker stops close to the source.

Figure 15 shows a second example of a successful track in which the cross-stream steering component is active. A single full cross-stream step is performed with subsequent adjustments of the cross-stream position due to the steering algorithm. The contrast threshold is based on the ratio of the signal acquired at the two outboard sensors. Cross-stream motion is activated when the average spike magnitude on one of the steering probes exceeds the value on the other probe by

a factor of *R*. The performance of the cross-stream steering algorithm is strongly affected by the threshold of the contrast measure. The practical range for the threshold for the ratio is R = 1.5 to 3.0. Smaller threshold values lead to more oscillatory paths, and larger threshold values lead to behaviour that does not react to important contrast events. For the track shown in Figure 15, the contrast measure threshold is R = 2.0. Figures 14 and 15 reveal that starting from the distance about 50 cm from the plume source the motion becomes straight with minimal side-to-side movements. This suggests that the algorithm does a good job of remaining centred on the plume once the cross-stream adjustments find the near centreline location.

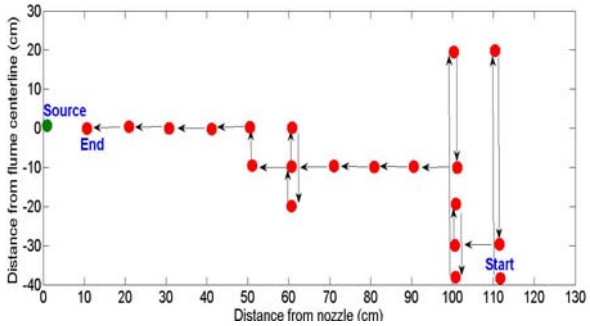

Figure 14. Example of a successful sensor-mediated track to the plume source. The time period of each step is typically 3.5 s. The full cross-stream sweeps take longer, roughly 20 s.

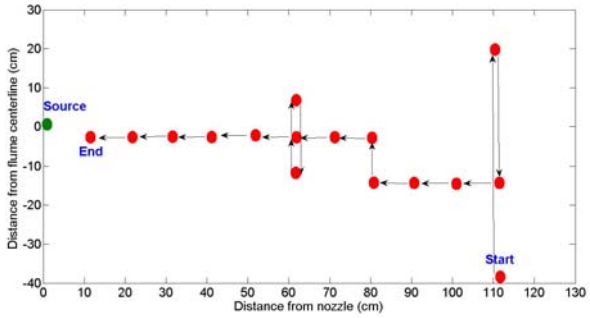

Figure 15. Example of a successful sensor-mediated track to the plume source.

Twenty-seven trails have been performed with the plume characteristics defined in the Methods section. For each trial, the initial distance of the tracker from the source was 114 cm. Of these trials, twenty-one tracks are declared as successful at autonomously moving toward the source and stopping in near proximity. The average final distance from the plume source location for the successful trials is 17.8 cm. The tracking period of the successful trails is 201 ± 43 s (mean ± std dev). During the tracks, 52% of the period is spent performing cross-stream motion, 37% of the period is spent moving upstream, and 11% of the period is spent stopped.

CONCLUSIONS

It is satisfying that the preliminary tracking trials demonstrated a high degree of success. With nearly 80% of the trials stopping near the source location, it is clear that the basic elements of the biologically-inspired algorithm design are a good foundation to build on as we refine and improve the algorithm. In particular, the implementation of the binary response to supra-threshold signal (to induce upstream movement) appears to yield sensory-mediated tracking behaviour that is consistent with blue crab behaviour. Source location percentage compares favourably to blue crab trackers, which typically locate odorant sources 60-75% of the time under similar conditions. While the tracking period is fairly rapid (order of 3 minutes), it still is much longer than that displayed by blue crabs, which require only ca. 30 s to track a similar distance. Hence, there is significant room for improved performance. Specific features of the algorithm that we plan to implement include adaptive response to the stimulus, including context-dependent speed and acceleration. This involves implementing the *Neuroadaptive Learning-Based Command Generator* element, which is currently not active. Further, the step size is currently very coarse (i.e., 10 cm), particularly in the cross-stream direction. Hence, we plan to implement much finer step size in the algorithm. The summary conclusion based on the preliminary trials is that adaptive responses allow for a set of simple rules to be used in a context-dependent manner to successfully track to a near source location. The algorithm is highly robust to changing environmental conditions without the need to fine tune the response thresholds *a priori* since the appropriate thresholds are extracted from the signal itself.

ACKNOWLEDGEMENTS

The authors thank the U.S. Defense Advanced Research Projects Agency (DARPA) for financial support under award number HR0011-10-1-0063.

REFERENCES

Crimaldi, J. P., Wiley, M. B., and Koseff, J. R., 2002, "The Relationship between Mean and Instantaneous Structure in Turbulent Passive Scalar Plumes", *J. Turbulence*, Vol. 3 (014), pp. 1-24.

Dickman, B. D., Webster, D. R., Page, J. L., and Weissburg, M. J., 2009, "Three-dimensional Odorant Concentration Measurements around Actively Tracking Blue Crabs", *Limnol. Oceanogr. Methods*, Vol. 7, pp. 96-108.

Farrell, J. A., Pang, S., and Li, W., 2005, "Chemical Plume Tracing via an Autonomous Underwater Vehicle", *IEEE J. Oceanic Engng.*, Vol. 30, pp. 428-442.

Grasso, F. W., Consi, T. R., Mountain, D. C., and Atema, J., 2000, "Biomimetic Robot Lobster Performs Chemo-orientation in Turbulence Using a Pair of Spatially Separated Sensors: Progress and Challenges", *Robotics and Autonomous Systems*, Vol. 30, pp. 115-131.

Ishida, H., Kobayashi, A., Nakamoto, T., and Moriizumi, T., 1999, "Three-dimensional Odor Compass", *IEEE Transactions on Robotics and Automation*, Vol. 15, pp. 100-106.

Jackson, J. L., Webster, D. R., Rahman, S., and Weissburg, M. J., 2007, "Bed Roughness Effects on Boundary-layer Turbulence and Consequences for Odor Tracking Behavior of Blue Crabs (*Callinectes sapidus*)", *Limnol. Oceanogr.*, Vol. 52, pp. 1883-1897.

Keller, T. A., Powell, I., and Weissburg, M. J., 2003, "Role of Olfactory Appendages in Chemically Mediated Orientation of Blue Crabs", *Mar. Ecol. Prog. Ser.*, Vol. 261, pp. 217-231.

Moore, P. A., and Atema, J., 1991, "Spatial Information Contained in Three-Dimensional Fine Structure of an Aquatic Odor Plume", *Biol. Bull.*, Vol. 181, pp. 408-418.

Page, J. L., Dickman, B. D. Webster, D. R., and Weissburg, M. J., 2011a, "Getting Ahead: Context-dependent Responses to Odor Filaments Drives Along-stream Progress during Odor Tracking in Blue Crabs", *J. Exp. Biol.*, Vol. 214, pp. 1498-1512.

Page, J. L., Dickman, B. D. Webster, D. R., and Weissburg, M. J., 2011b, "Staying the Course: Chemical Signal Spatial Properties and Concentration Mediate Cross-stream Motion in Turbulent Plumes", *J. Exp. Biol.*, Vol. 214, pp. 1513-1522.

Rahman, S., and Webster, D. R., 2005, "The Effect of Bed Roughness on Scalar Fluctuations in Turbulent Boundary Layers", *Exp. Fluids*, Vol. 38, pp. 372-384.

Webster, D. R., 2007, "The Structure of Turbulent Chemical Plumes", in *Trace Chemical Sensing of Explosives*, R .L. Woodfin, ed., Wiley-Interscience, Hoboken, N.J., pp. 109-129.

Webster, D. R., Rahman, S., and Dasi, L. P., 2003, "Laser-induced Fluorescence Measurements of a Turbulent Plume", *ASCE J. Engineering Mech.*, Vol. 129, pp. 1130-1137.

Webster, D. R., and Weissburg, M. J., 2001, "Chemosensory Guidance Cues in a Turbulent Chemical Odor Plume", *Limnol. Oceanogr.*, Vol. 46, pp. 1034-1047.

Webster, D. R., and Weissburg, M. J., 2009, "The Hydrodynamics of Chemical Cues among Aquatic Organisms", *Annual Review of Fluid Mechanics*, Vol. 41, pp. 73-90.

Weissburg, M. J., and Dusenbery, D. B., 2002, "Behavioral Observations and Computer Simulations of Blue Crab Movement to a Chemical Source in a Controlled Turbulent Flow", *J. Exp. Biol.*, Vol. 205, pp. 3387-3398.